Published in final edited form as:
Biomaterials. 2011 April ; 32(10): 2605–2613. doi:10.1016/j.biomaterials.2010.11.073.

The effect of internalizing human single chain antibody fragment on liposome targeting to epithelioid and sarcomatoid mesothelioma

Arun K. Iyer[1], **Yang Su**[2], **Jinjin Feng**[1], **Xiaoli Lan**[1], **Xiaodong Zhu**[2], **Yue Liu**[2], **Dongwei Gao**[1], **Youngho Seo**[1], **Henry F. VanBrocklin**[1,3], **V. Courtney Broaddus**[3,4], **Bin Liu**[2,3], and **Jiang He**[1,3,*]

[1]Center for Molecular and Functional Imaging, Department of Radiology and Biomedical Imaging, University of California at San Francisco, San Francisco, CA 94143

[2]Department of Anesthesia, University of California at San Francisco, San Francisco, CA 94110

[3]UCSF Helen Diller Family Comprehensive Cancer Center, San Francisco, CA 94143

[4]Lung Biology Center, Department of Medicine, University of California at San Francisco, San Francisco, CA 94143

Abstract

Immunoliposomes (ILs) anchored with internalizing human antibodies capable of targeting all subtypes of mesothelioma can be useful for targeted imaging and therapy of this malignant disease. The objectives of this study were to evaluate both the *in vitro* and *in vivo* tumor targeted internalization of novel internalizing human single chain antibody (scFv) anchored ILs on both epithelioid (M28) and sarcomatoid (VAMT-1) subtypes of human mesothelioma. ILs were prepared by post-insertion of mesothelioma-targeting human scFv (M1) onto preformed liposomes and radiolabeled with ^{111}In (^{111}In-IL-M1), along with control non-targeted liposomes (^{111}In-CL). Incubation of ^{111}In-IL-M1 with M28, VAMT-1, and a control non-tumorigenic cell-line (BPH-1) at 37°C for 24 h revealed efficient binding and rapid internalization of ILs into both subtypes of tumor cells but not into the BPH-1 cells; internalization accounted for approximately 81-94% of total cell accumulation in mesothelioma cells compared to 37-55% in control cells. In tumor bearing mice intravenous (i.v.) injection of ^{111}In-IL-M1 led to remarkable tumor accumulation: 4 % and 4.7% injected dose per gram (% ID/g) for M28 and VAMT-1 tumors, respectively, 48 h after injection. Furthermore, tumor uptake of ^{111}In-IL-M1 in live xenograft animal models was verified by single photon emission computed tomography (SPECT/CT). In contrast, i.v. injection of ^{111}In-CL in tumor-bearing mice revealed very low uptake in both subtypes of mesothelioma, 48 h after injection. In conclusion, M1 scFv-anchored ILs showed selective tumor targeting and rapid internalization into both epithelioid and sarcomatoid subtypes of human mesothelioma, demonstrating its potential as a promising vector for enhanced tumor drug targeting.

[*]**Correspondence should be addressed to:** Jiang He, PhD Center for Molecular and Functional Imaging Department of Radiology and Biomedical Imaging University of California at San Francisco 185 Berry Street, Suite 350 San Francisco, CA 94143 Tel: 415-3533638; Fax: 415-5148242 Jiang.He@ucsf.edu.

Movie File. Three-dimensional SPECT/CT movie of radiolabeled targeted immunoliposome (^{111}In-IL-M1$_{(50)}$) uptake in mice bearing both epithelioid (M28) and sarcomatoid (VAMT-1) tumors, 24 h post injection is shown.

Keywords

Immunoliposomes; scFv antibody; mesothelioma; SPECT/CT imaging; tumor targeting

1. Introduction

Malignant mesothelioma is a deadly cancer without a current curative treatment [1,2]. Mesothelioma develops from the mesothelium—a protective membrane that covers many of the body's internal organs, decades after exposure to asbestos [3-5]. Histologically, mesothelioma is categorized into three major subtypes: epithelioid, sarcomatoid and biphasic (or mixed) mesothelioma [6-8]. The diagnosis of mesothelioma is often delayed because the symptoms are similar to other conditions. Mesothelioma in general has a poor prognosis. The response to treatment is limited and varies with the subtype and stage of the disease; for instance patients diagnosed with the more aggressive sarcomatoid mesothelioma are often less likely to respond to treatment than those with epithelioid mesothelioma [9,10]. With ongoing exposure to asbestos in the community and with populations already known to be at risk, there is an urgent unmet need to develop new strategies for early diagnosis and treatment of mesothelioma, irrespective of their subtype or origin.

One promising approach for treating mesothelioma is by utilizing nanotechnology to develop multifunctional nanocarriers [11]. Among the several nanocarriers that are available for drug delivery, liposomes have been extensively studied and are FDA-approved as a safe material for drug delivery applications [12]. In this regard, PEGylated liposomes are ideally suited because of their favorable pharmacokinetic profiles and long plasma half-life *in vivo* [13,14]. Also, nanosized liposomes can take advantage of the enhanced permeability and retention (EPR)-effect for tumor drug targeting making them versatile carriers for targeted anticancer therapy [15,16]. Moreover, liposome's can be easily tailored to encapsulate therapeutic payloads as well as surface functionalized with multifunctional agents such as targeting ligands, antibodies, peptides and/or radiotracers for simultaneous imaging/ detection and therapeutic applications [11,17-19].

In order to develop multifunctional immunoliposomes (ILs), as a therapy aimed at mesothelioma, the first step would involve development of ligands or of antibodies that can selectively target overexpressed receptors or antigens on mesothelioma tumor cells. Along these lines, we have identified a panel of internalizing human single chain (scFv) antibodies that can not only target cell surface antigens associated with both epithelioid and sarcomatoid subtypes of human mesothelioma [20] but also internalize rapidly into mesothelioma tumor cells. Also, we showed that these scFvs bind to mesothelioma tumors *ex vivo*, thereby recognizing clinically represented tumor antigens [20] and offer the potential to target tumor cells selectively [21]. More importantly, we have recently identified melanoma cell adhesion molecule (MCAM/CD146/MUC18) as a target antigen for mesothelioma tumor cells by screening the yeast surface human cDNA display library with mesothelioma targeting phage antibody [21]. MCAM was overexpressed in more than 80% of epithelioid and sarcomatous mesothelioma tissues, but was not highly expressed in normal mesothelial tissues [21]. Recently, we also showed that one of the scFv identified by phage display library (M40) radiolabeled with ^{99m}Tc (^{99m}Tc-M40) could selectively target and internalize rapidly into both epithelioid and sarcomatoid mesothelioma *in vitro* and *in vivo* and the tumors could be clearly visualized by small animal-SPECT/CT (Iyer *et al.*, unpublished results).

In the current study, we have utilized the targeting and rapid internalizing function of one the scFv (M1) by conjugating them to liposomes, to form target-internalizing ILs. As a

further translation of these ILs for clinical development, we have investigated both the *in vitro* and *in vivo* tumor targeting and imaging of the internalizing human single chain antibody fragment (M1 scFv) anchored ILs radiolabeled with ^{111}In (^{111}In-IL-M1) on both epithelioid (M28) and sarcomatoid (VAMT-1) subtypes of human mesothelioma.

2. Materials and methods

2.1. Materials

All the lipids and their derivatives such as 1-hexadecanoyl-2-(9Z-octadecenoyl)-*sn*-glycero-3-phosphocholine (POPC), (1,2dimyristoyl-*sn*-glycero-3-phospho-ethanolamine-N-diethylene-triamine-pentaaceticacid) (DMPE-DTPA), 1,2-distearoyl-*sn*-glycero-3-phosphoethanolamine-N-[amino(polyethyleneglycol)-2000]) (DSPE-mPEG$_{2000}$), and 1,2-distearoyl-*sn*-glycero-3-phospho-ethanolamine-N-[maleimide(polyethyleneglycol)-2000] (DSPE-PEG$_{2000}$-MAL) were purchased from Avanti Polar Lipids (Alabaster, AL). Cholesterol obtained from Sigma-Aldrich Chemical Co., (St. Louis, MO) was recrystallized in methanol before use. Dry chloroform, DMSO (anhydrous) and phosphate buffer saline (10X PBS) were purchased from Sigma-Aldrich Chemical Co., (St. Louis, MO). 2-mercaptoethanolamine (2-MEA) was obtained from Pierce Biotechnology (Rockford, IL). A mini-extruder was purchased from Avanti Polar Lipids Inc., (Alabaster, AL), with Whatman® polycarbonate membrane filter accessories for extrusion of the liposomes. PD-10 columns (Sephadex G-25) and Sepharose GL-4B-10 were purchased from GE Healthcare (Buckinghamshire, UK). $^{111}InCl_3$ was obtained from Perkin Elmer life Science Inc., (Boston, MA).

2.2. Production of M1 scFv targeting mesothelioma

To produce soluble scFvs (M1), genes encoding the scFvs were spliced into an expression vector imparting a c-myc epitope and a hexahistidine tag at the carboxy terminus [22]. To produce soluble cysteine tagged scFvs (M1-CH), a second vector was used to impart a cysteine residue and a hexahistidine tag at the carboxy terminus [22]. Antibody fragments were harvested from the bacterial periplasmic space and purified by immobilized metal affinity chromatography and gel filtration as described before [22]. Following overnight dialysis in phosphate buffer saline (PBS), the antibody purity was determined by gel electrophoresis and its concentration was determined using a UV spectrometer (NanoDrop Products/Thermo Scientific, Wilmington, DE) by quantifying the absorbance at 280 nm.

2.3. Preparation of liposomes

Liposomes were prepared by thin lipid film hydration followed by sonication and extrusion as reported by MacDonald et al., [23] with modifications. Briefly, liposomes composed of a room temperature transition lipid (POPC), cholesterol, DSPE-mPEG$_{2000}$, and DMPE-DTPA, were combined in a molar ratio of 200:133:0.1:0.03 respectively. A thin lipid film was formed by evaporating the solvent on a rotary evaporator (Labrota 4000, Heidolph Instruments GmbH, Schwabach, Germany) under vacuum in a 10 ml round bottom flask. The lipid layer was further subjected to overnight drying in a vacuum desiccator. Each liposome batch consisted of 50 μmole/L phospholipid and was rehydrated in 1X PBS (pH 7.4). Hydration of the lipid films was done at room temperature, involving vigorous vortexing (Vortex-Genie, Scientific Industries, Bohemia, NY) for 15 min., followed by sonication (2510 Bransonic, Branson Ultrasonics, Danbury, CT) for 1 h. The resulting multi-lamellar liposomes were repeatedly extruded (11 times) at room temperature through Whatman® polycarbonate membranes filters of gradually decreasing pore size of 0.8, 0.4, 0.2, 0.1 and 0.08 μm respectively, using a mini-extruder, yielding unilamellar liposomes of ~100 nm diameter. The hydrodynamic diameter of the liposomes was determined by dynamic light scattering (Malvern Instruments, Southborough, MA) and the ζ potentials

were determined with a Malvern Zetasizer IV (Malvern Instruments, Southborough, MA). The phospholipid concentration of the liposome was determined by a phosphorous assay as described [24].

2.4. Preparation of scFv anchored immunoliposomes

2.4.1. Reduction of M1 scFv—The reduction of cysteine residues in the scFv (M1-CH) was performed using a standard procedure provided by the manufacturer (Pierce Biotechnology, Rockford, IL). Briefly, 100 μl (6 mg/ml) of M1-CH, was mixed with 1.5 μl EDTA (0.5 M, pH 8.5) and 11 μl of a 2-MEA (20 mmol/L, 6 mg/100 μl stock solution). The reaction was allowed to proceed at 37°C for 1.5 h. The efficiency of cysteine reduction was assayed using Ellmann's reagent, and was typically >90%. Subsequently, the reduced antibody was purified using Sephadex G-25 column chromatography (PD-10, GE Healthcare), equilibrated with 0.1 M $NaHCO_3$/1 mM EDTA buffer (pH 8.0). The purified fraction was concentrated by using a centrifugal filtration device (Millipore, Milford, MA) with 10 kDa molecular weight cut-off (MWCO) filter, at 3000 rpm for 15 min., and the final concentration of scFv was determined using a UV spectrometer (NanoDrop Products/ Thermo Scientific, Wilmington, DE), as well as a BCA protein assay kit (Pierce Biotechnology, Rockford, IL).

2.4.2. Conjugation of reduced M1-CH scFv with Mal-PEG_{2000}-DSPE—The reduced M1-CH scFv were conjugated to Mal-PEG-DSPE as described [25,26]. Briefly, a stock solution of MAL-PEG_{2000}-DSPE (20 mg/ml) was first prepared using dry DMSO. A 5 μl MAL-PEG_{2000}-DSPE stock solution was reacted with 100 μl (200 μg) of the reduced ScFv in 0.1 M $NaHCO_3$/1 mM EDTA buffer (pH 8.0), corresponding to 5:1 molar excess of maleimide groups to that of reduced scFv. The conjugation reaction was carried out for 1.5 h at room temperature. Subsequently, Sephadex G-25 column chromatography (PD-10, GE Healthcare) was performed to purify the conjugate and exchange the buffer to 1X PBS (pH 7.4). Purified fractions were pooled and concentrated by using Amicon® Ultra-4 centrifugal filtration device (Millipore, Milford, MA) with a 10 kDa MWCO filter. This process resulted in formation of an active surface for conjugation of the scFvs to the liposomes.

2.4.3. Preparation of immunoliposomes—To obtain ILs, the insertion of the scFv conjugated PEG (DSPE-PEG_{2000}-M1) onto preformed liposomes was performed by employing a post-insertion technique [27]. ILs were prepared with varied antibody density ranging from 1 to 200 antibody molecules *per* vesicle. For this purpose varied concentration of liposome (lipid) in (0.01 M PBS) was incubated with fixed amount of DSPE-PEG_{2000}-M1 scFv for 1 h (as shown in Table 1), under mild rotation using a rotary evaporator (Labrota 4000, Heidolph Instruments GmbH, Schwabach, Germany) without applying vacuum. As a result, the conjugates become attached to the outer lipid layer of the vesicles *via* hydrophobic DSPE domains. The purification of scFv-anchored ILs from the unconjugated scFvs (DSPE-PEG_{2000}-M1) was performed using a Sepharose CL-4B-10 (GE Healthcare) gel chromatography using 1X PBS as the mobile phase.

2.5. Radiolabeling of control liposome and immunoliposomes with ^{111}In

For the purpose of radiolabeling the liposomes, typically 0.5-1.0 mCi (18.5-37 MBq) of ^{111}In was used. 15 μl (0.05 N HCl) of $^{111}InCl_3$ (Perkin Elmer Inc., Boston, MA) was taken in an eppendorf tube and 9 μl of 0.5 M sodium acetate was added to adjust the pH to ~5.5 - 6.0. Then 100 μl of the control (non-targeted) liposomes or ILs was added to the eppendorf tube and incubated for 1 h at room temperature. Subsequently, Sephadex G-25 (GE Healthcare) column chromatography using PBS as the mobile phase was performed to purify the ^{111}In labeled control liposomes or ILs. Both size exclusion-chromatography (Waters Corp., Milford, MA) and radio-thin layer chromatography (TLC) (Bioscan Radio-

TLC Imaging Scanner, Bioscan Inc., Washington DC) were used to characterize the ^{111}In labeled CLs (^{111}In-CL) or ILs (^{111}In-IL-M1) for labeling efficiency, purity as well as for assessing the *in vitro* stability of the radiolabeled liposomes in buffers and serum. In the case of radio-TLC, the macromolecular ^{111}In-CL or ^{111}In-IL-M1 remain at the original loading position whereas the unbound radioligand migrates with the solvent front. The labeling efficiency was estimated from the ratio of radioactivity at the origin compared to the total applied.

2.6. In vitro cell binding and internalization studies

1 million M28, VAMT-1, or control non-tumorigenic (BPH-1) cells were suspended in RPMI-1640 media with 10% fetal bovine serum at 37°C. Approximately 150 kBq ^{111}In-labeled ILs (^{111}In-IL-M1) in a final concentration ranging from 1 nmol/L to 80 nmol/L were added to the cell suspensions and incubated at 37°C in 5 % CO_2 for 24 h. After 24 h, the cells were resuspended, washed twice with ice-cold PBS (pH 7.2) and then washed twice with ice-cold glycine buffer (0.05 mol/L glycine solution, 150 mmol/L NaCl, pH adjusted to 2.8 with 1 N HCl) to distinguish between cell surface-bound (acid releasable) and internalized (acid resistant) radioligand. Finally, cells were lysed with 1 N NaOH at 37°C for 10 min. The radioactivity in the cells were measured by using a gamma counter (Wizard, Perkin Elmer, Milwaukee, WI) and expressed as the percentage of applied activity normalized to 1 million cells.

2.7. Animal studies

Animal procedures were performed according to a protocol approved by University of California, San Francisco, Institutional Animal Care and Use Committee.

2.7.1. Xenograft model—Six-week-old male *nu/nu* mice were purchased from Charles River Laboratories (Wilmington, MA). For tumor inoculation, 1 million M28 and VAMT-1 cells in 200 μL of PBS were administered subcutaneously to seed tumor growth into the right and left shoulders of the animal respectively. Growing tumors were palpated, and the diameters were measured by a vernier caliper. The experiments were commenced when tumor size reached ~3-5 mm in diameter.

2.7.2. Biodistribution studies—Tumor-bearing nude mice in groups of 4 animals were injected intravenously (i.v.) with 18.5–37 MBq (0.5-1.0 mCi) of ^{111}In-IL-M1 or ^{111}In-CL. The mice were euthanized and dissected at 24 h or 48 h after injection of ILs or CLs. Blood, tumor, and major organs were harvested and weighed. The radioactivity in the tissues was measured using a gamma-counter (Wizard, Perkin Elmer, Milwaukee, WI). The results are presented as percentage injected dose per gram (%ID/g) of tissue/organ.

2.8. SPECT/CT imaging

Mice were imaged with a dedicated small animal SPECT/CT system (FLEX X-SPECT/X-O, Gamma Medica-Ideas, Inc., Northridge, CA). For anatomical correlation, the CT was first performed after 18.5–37 MBq of ^{111}In-labeled liposomes was injected intravenously. As a general procedure, the mouse was placed in the mouse bed and positioned in front of a 2.0 mm diameter pinhole collimator designed for high energy photons (171 and 245 keV) emitted by ^{111}In. The spatial resolution and sensitivity of the pinhole SPECT system had been characterized from phantom studies and for this imaging geometry, the system spatial resolution was 2.0 mm with a sensitivity of 4,600 counts/min/MBq (170 counts/min/μCi). A planar image of the line source attached to the holder was acquired for post-acquisition correction of misalignment error. SPECT imaging was initiated 24-48 h after injection of the radiolabeled liposomes, and 64 projection views were acquired over a 360° angle rotation in

a 80×80 matrix. The acquisition time ranged from 30 s/projection to 60 s/projection for a total of 0.5 to 1 h approximately.

2.9. Statistical Analysis

All quantitative data are reported as mean ± SD. Statistical analysis was performed using a Student's t-test and with more than two data sets, ANOVA was used to compare results. Data were considered as statistically significant for P values of 0.05 or less.

3. Results

3.1. Preparation of liposomes and immunoliposomes

For the preparation of liposomes and ILs the use of room temperature transition POPC lipid was advantageous because the extrusion process to form unilamellar liposomes could be carried out at room temperature. The process of sonication and extrusion of lipid films resulted in formation of unilamellar vesicles of ~100 nm size. Measurement of the hydrodynamic diameter of the control non-targeted liposome (CL) by dynamic light scattering showed that the size was 97.3 ± 4.60 nm (Table 2). For the preparation of ILs a post insertion technique was used [27]. The cysteine residues on the scFv were first reduced for facilitating the conjugation of the scFv to DSPE-PEG-maleimide. The efficiency of cysteine reduction was >90% as assayed by Ellmann's reagent [28]. The conjugation of reduced scFv to DSPE-PEG-maleimide resulted in an active surface for insertion of scFv onto the liposome vesicle. Typically 80-85% of the added scFv conjugate (DSPE-PEG-M1) was incorporated into ILs as observed by BCA protein assay, performed after insertion and purification of the ILs. As seen in Table 2., the hydrodynamic size of the ILs increased from ~100 nm (for the control non-targeted liposomes) to 109.7± 3.86 nm, for liposomes inserted with ~50 scFv *per* vesicle. The size further increased to 117.3± 3.35 nm when the scFv number was increased to 100 *per* vesicle indicating the successful attachment of the scFvs to the liposomes thereby forming targeted ILs.

For facilitating radiolabeling of CLs and ILs, a DTPA-conjugated lipid (DMPE-DTPA) was incorporated during liposome fabrication similar to the one reported earlier [29]. The radiolabeling efficiency was >98% for both the ^{111}In-CL and ^{111}In-IL-M1 as determined by radio-TLC and size exclusion chromatography (SEC), indicating the successful labeling of the liposomes. Also, SEC revealed that the liposomal formulation were stable and eluted as a single peak when incubated in 0.01 M phosphate buffer saline (pH 7.4) or 10 % serum at 37°C for up to 36 h (data not shown). The hydrodynamic size of the liposomes also remained unaltered (~100 nm) during storage for up to 1 week at room temperature or up to one month at 4°C as determined by dynamic light scattering (data not presented).

3.2. In vitro cell binding and internalization studies

In order to determine the *in vitro* cell binding and internalization potentials of the M1-ScFv conjugated ILs, varied density of ScFv *per* vesicle was inserted onto ^{111}In labeled liposomes (as shown in Table 1.) and incubated with a sarcomatoid mesothelioma (VAMT-1) cell line which previously showed rapid and selective binding and internalization of a ^{99m}Tc-labeled M1 scFv during a preliminary random antibody library screening [20]. From the results (Figure 2), it can be seen that at the tested concentration of liposomes (from 1 nM to 60 nM of lipid), as the density of ScFv per vesicle increased, the internalization of the ^{111}In labeled M1-ILs also increased until about 50-60 ScFv *per* vesicle and above this threshold number, the internalization of ILs plateaued, and the binding/internalization remained almost constant (Figure 2).

In the next study we investigated the effect of concentration of lipid (liposome) on both the binding and internalization of ^{111}In-IL-M1$_{(50)}$ having an optimal scFv density of ~50 *per* vesicle in both epithelioid (M28) and sarcomatoid mesothelioma (VAMT-1) cells. The results were compared with a control non-tumorigenic cell line (BPH-1) as shown in Figure 3. It can be seen from Figure 3 that after 24 h incubation of ^{111}In-IL-M1$_{(50)}$ at all the lipid concentrations tested (from 1 nM to 60 nM), the total amount (% of total) bound and the total amount internalized was much higher (>85%) for both the mesothelioma cells in comparison to the control non-tumorigenic (BPH-1) cells (<35%). It is also interesting to note that for the case of mesothelioma cells, the ratio of internalized component versus total bound component (% of total radioactivity) was ~90 (Figure 4 B) indicating that a majority of the ILs that bound to the tumor cells were rapidly internalized into the cells.

3.3. Small animal SPECT/CT imaging and biodistribution of ^{111}In-labeled immunoliposomes

The ^{111}In-IL-M1$_{(50)}$ formulation containing an optimal number of ~50 scFv *per* vesicle was used to investigate the *in vivo* tumor targeted imaging and biodistribution of mice bearing both epithelioid (M28) and sarcomatoid (VAMT-1) mesothelioma tumor xenografts. The grafting of the two different subtypes of mesothelioma tumors (M28 and VAMT-1) in a single animal was useful in visualizing (and comparing) the tumor uptake of the radiolabeled ILs in both the tumor subtypes simultaneously, using SPECT/CT. The result of SPECT/CT imaging using live xenograft mice model is shown in Figure 5. It can be seen from the image taken 24 h post injection that the ^{111}In-IL-M1$_{(50)}$ showed marked uptake into both M28 and VAMT-1 mesothelioma tumors. There was also high uptake in the liver and the spleen. The imaging results corroborated the *ex vivo* biodistribution studies performed 24 and 48 h after injection of the ^{111}In-IL-M1$_{(50)}$ (Table 3, Figure 6 and 7). It can seen from the Table 3 and Figure 6 and 7 that ^{111}In-IL-M1$_{(50)}$ was cleared from most normal organs (except the liver and the spleen), giving M28 and VAMT-1 tumors to blood ratios of 31:1 and 36:1 and tumor to muscle ratios of 47:1, 55:1 respectively at 48 h after injection. More importantly, at 48 h after injection there was markedly high and almost comparable tumor uptake of 4.01±0.39 and 4.69±0.72 % ID/g of tissue for M28 and VAMT-1 tumors respectively, which were much higher than all organs/tissues studied (except the liver 7.97±0.34) (Table 3 and Figure 6). In contrast, the control study using non-targeted liposome (^{111}In-CL) exhibited tumor uptake of only 0.97±0.48 and 0.4±0.42% %ID/g for M28 and VAMT-1 tumors respectively (Table 1, Figure 7).

4. Discussion

Malignant mesothelioma is a deadly tumor that currently has no curative treatment option [2,30]. A few earlier studies using non-targeted liposomes were found useful for treating mesothelioma in the clinic [31-34]. Moreover, current developments using immunoliposomes (ILs) have shown promise for targeted anti-cancer therapies [35-40]. In this report we have focused our attention on developing ILs anchored with internalizing (M1) scFvs and investigated both their *in vitro* and *in vivo* tumor targeted binding and internalization towards two different subtypes of human mesothelioma, derived from epithelioid (M28) and sarcomatoid (VAMT-1) origins.

The composition of the liposomes and the method of their fabrication, as well as their stability are some of the important parameters that have to be tailored for particular drug delivery application [41-43]. In this regard, our liposomes showed good *in vitro* stability in PBS or serum at 37°C up to 72 h and their size remained unaltered (~100 nm) on storage up to 1 month at 4°C (data not shown).

For the IL preparation, we used a method of first conjugating the scFv at the distal end of PEG_{2000} chains (before insertion onto the surface of liposomes) instead of direct labeling of the scFv onto the liposomes (Figure 1), based on favorable results reported earlier [44-46]. For the scFv conjugation reaction, ideally we want to achieve close to 100 % coupling efficiencies without altering its binding affinity. We thus engineered the scFv to contain a cysteine tag that could conveniently be reduced and conjugated to DSPE-PEG functionalized with a maleimide linker (DSPE-PEG_{2000}-MAL) [47].

We used a simple yet effective post-insertion technique for conjugating the DSPE-PEG_{2000}-scFv onto the surface of the liposomes, to form targeted ILs [48]. In this regard, our room temperature insertion technique helped preserve the affinity of the scFvs, contrary to the post-insertion method which usually involves exposing the antibody to elevated temperatures (usually ~60°C for 1 h), where the potential exists, for detrimental effects on the antibody, such as reduction in its binding affinity for its target antigen [27].

It has been predicted [49] and experimentally demonstrated that the apparent affinity of multivalent ILs can be several fold higher than that of their monovalent counterparts [50]. We thus first optimized the scFv density on the surface of liposomes (Table 1 and Figure 2). We observed that increasing the antibody density on the liposome surface increased the binding affinity, and in turn the internalizing ability of the ILs to the target cells (Figure 2), consistent with what was observed for similar systems [51,52]. While IL binding to cells with different amounts of surface antigen may vary, antibody densities of ~50 scFv *per* vesicle was found optimal in our case (Figure 2). Our current findings and prior reports indicate that larger amounts of bound antibody may not be necessary for efficient target binding of scFvs to cells [53,54]. More interestingly, a detailed *in vitro* cell binding and internalization study using the optimized ILs (^{111}In-IL-$M1_{(50)}$) revealed not only efficient and selective binding but also rapid internalization of the ILs by both epithelioid (M28) and sarcomatoid (VAMT-1) mesothelioma cells, but not by the non-targeted BPH-1 cells (Figure 3 and 4). In contrast, we observed that the *in vitro* cell binding and internalization of ^{111}In-CL under varied lipid concentrations was comparably much lower (<40%) in all the three (M28, VAMT-1 and BPH-1) cell lines, under identical conditions, even after 48 h of incubation (data not shown).

Although the findings from the *in vitro* cell studies using ^{111}In-IL-$M1_{(50)}$ are very encouraging, it is essential to test the ILs *in vivo* on animal tumor models for successful translation into clinics. As a next step in this direction, we tested the ^{111}In-IL-$M1_{(50)}$ on xenograft mice models bearing both epithelioid (M28) and sarcomatoid (VAMT-1) mesothelioma. The live animal imaging using SPECT/CT and *ex vivo* biodistribution results corroborated the *in vitro* findings. For instance, we observed that the uptake of ^{111}In-IL-$M1_{(50)}$ in both M28 and VAMT-1 tumors was strikingly high in the time frame of our study, higher than all other organs/tissues studied (except the liver 7.97±0.34) (Table 3 and Figure 5) and the tumors could be clearly visualized by SPECT/CT (with values of 4.01±0.39 and 4.69±0.72 % ID/g for M28 and VAMT-1 tumors respectively at 48 h after injection). From the Figures 6 and 7, it can be noted that for the time frame from 24 h to 48 h the clearance of the ^{111}In-IL-$M1_{(50)}$ from most of the non-target organs and tissues occurred rapidly whereas the tumor uptake remained high, even at 48 h time point. This result may be attributed to the efficient binding and rapid internalization of the ^{111}In-IL-$M1_{(50)}$ into the tumor cells.

It should be noted that we intentionally used a low % of PEG in our liposome formulations in order distinguish the internalizing property and the 'active tumor targeting' ability of the ^{111}In-IL-$M1_{50}$ in comparison to the ^{111}In-CL. From our results it is clear that the ^{111}In-IL-$M1_{(50)}$ showed much higher tumor targeted uptake in comparison to ^{111}In-CL (Figure 5, 6 and 7, Table 3). It can also be observed that the lower % PEGylation of ^{111}In-IL-$M1_{(50)}$

may have attributed at least in part for their faster clearance from the blood as early as 24 h (Figure 6), thus providing a good contrast for early tumor imaging by SPECT/CT (Figure 5). However the lower % PEGylation also resulted in shorter plasma circulation half-life of ^{111}In-IL-M1$_{(50)}$. Hence, further optimization of the ILs using higher % PEG may render longer plasma half-life to the ILs thereby facilitating their preferential accumulation in the target tumors by passive targeting strategies or the EPR-effect [15,16]. Furthermore, the stealth ILs may also help evade the RES, thereby reducing its in non-target uptake in organs such as the liver and the spleen [55,56].

Although we have addressed some of the critical issues of the ILs *in vitro* in cell cultures and *in vivo on* animal models, there still remain several questions regarding their effective use in the clinical settings. For instance while our cell studies and animal model demonstrates the ability of the ILs to target and internalize into the cells and implanted tumors *in vivo*, their ability to reach the target tissue/cell in the clinical setting may vary or depend on whether the target is accessible from the vasculature [53,57,58]. Also their *in vivo* stability and half life, tendency to evoke immune response or ability to effectively evade RES and reach their target organ/tissue are some of the other important factors that needs to be evaluated.

5. Conclusion

The preset study reveals that our internalizing M1 human scFvs anchored immunoliposomes showed selective tumor targeting and rapid internalization into both epithelioid (M28) and sarcomatoid (VAMT-1) subtypes of human mesothelioma *in vitro* and *in vivo* demonstrating its potentials as a promising vector for enhanced targeting of liposomal drugs and radionuclides for imaging and therapy of this malignant disease.

Supplementary Material

Refer to Web version on PubMed Central for supplementary material.

Acknowledgments

The authors wish to thank Prof. Francis C. Szoka, Jr., Department of Biopharmaceutical Sciences, UCSF, for permitting use of his facility for dynamic light scattering and zeta potential measurements. This work is partially supported by NIH R01 CA135358 and the American Cancer Society (IRG-97-150-10) to Jiang He, and R01 CA118919 and R01 CA129491 to Bin Liu.

References

1. Sterman DH, Recio A, Haas AR, Vachani A, Katz SI, Gillespie CT, et al. A Phase I Trial of Repeated Intrapleural Adenoviral-mediated Interferon-beta Gene Transfer for Mesothelioma and Metastatic Pleural Effusions. Mol Ther 2010;18:852–860. [PubMed: 20068553]
2. Curran D, Sahmoud T, Therasse P, Van Meerbeeck J, Postmus P, Giaccone G. Prognostic factors in patients with pleural mesothelioma: the European Organization for Research and Treatment of Cancer experience. J Clin Oncol 1998;16:145–152. [PubMed: 9440736]
3. Bianchi C, Bianchi T. Malignant mesothelioma: global incidence and relationship with asbestos. Ind Health 2007;45:379–87. [PubMed: 17634686]
4. Smith A, Wright C. Chrysotile asbestos is the main cause of pleural mesothelioma. Am J Ind Med 1996;30:252–266. [PubMed: 8876792]
5. Dunleavey R. Malignant mesothelioma: risk factors and current management. Nurs Times 2004;100:40–43. [PubMed: 15132064]

6. Churg, A.; Roggli, V.; Galateau-Salle, F.; Cagle, P.; Gibbs, A.; Hasleton, P., et al. Mesothelioma.. In: Travis, W.; Brambilla, E.; Muller-Hermelink, H.; Harris, C., editors. Pathology & Genetics Tumours of the Lung, Pleura, Thymus and Heart. IARC; Lyon: 2004. p. 125-136.
7. Attanoos R, Gibbs A. Pathology of malignant mesothelioma. Histopathology 1997;30:403–418. [PubMed: 9181361]
8. Ho L, Sugarbaker D, Skarin A. Malignant pleural mesothelioma. Cancer Treat Res 2001;105:327–373. [PubMed: 11224994]
9. Butchart E. Contemporary management of malignant pleural mesothelioma. Oncologist 1999;4:488–500. [PubMed: 10631693]
10. Klebe S, Brownlee N, Mahar A, Burchette J, Sporn T, Vollmer R, et al. Sarcomatoid mesothelioma: a clinical-pathologic correlation of 326 cases. Mod Pathol 2010;23:470–479. [PubMed: 20081811]
11. Torchilin V. Multifunctional nanocarriers. Adv Drug Deliv Rev 2006;58:1532–1555. [PubMed: 17092599]
12. Farokhzad O, Langer R. Nanomedicine: developing smarter therapeutic and diagnostic modalities. Adv Drug Deliv Rev 2006;58:1456–1459. [PubMed: 17070960]
13. Papahadjopoulos D, Allen T, Gabizon A, Mayhew E, Matthay K, Huang S, et al. Sterically stabilized liposomes: improvements in pharmacokinetics and antitumor therapeutic efficacy. Proc Natl Acad Sci U S A 1991;88:11460–11464. [PubMed: 1763060]
14. Allen T. Long-circulating (sterically stabilized) liposomes for targeted drug delivery. Trends Pharmacol Sci 1994;15:215–220. [PubMed: 7940982]
15. Maeda H, Wu J, Sawa T, Matsumura Y, Hori K. Tumor vascular permeability and the EPR effect in macromolecular therapeutics: a review. J Control Release 2000;65:271–284. [PubMed: 10699287]
16. Iyer AK, Khaled G, Fang J, Maeda H. Exploiting the enhanced permeability and retention effect for tumor targeting. Drug Discov Today 2006;11:812–818. [PubMed: 16935749]
17. Nielsen U, Kirpotin D, Pickering E, Hong K, Park J, Refaat Shalaby M, et al. Therapeutic efficacy of anti-ErbB2 immunoliposomes targeted by a phage antibody selected for cellular endocytosis. Biochim Biophys Acta 2002;1591:109–118. [PubMed: 12183061]
18. Kweon S, Lee HJ, Hyung WJ, Suh J, Lim JS, Lim SJ. Liposomes coloaded with iopamidol/lipiodol as a RES-targeted contrast agent for computed tomography imaging. Pharm Res 2010;27:1408–1415. [PubMed: 20424895]
19. Jiang J, Yang SJ, Wang JC, Yang LJ, Xu ZZ, Yang T, et al. Sequential treatment of drug-resistant tumors with RGD-modified liposomes containing siRNA or doxorubicin. Eur J Pharm Biopharm 2010;76:170–178. [PubMed: 20600887]
20. An F, Drummond D, Wilson S, Kirpotin D, Nishimura S, Broaddus V, et al. Targeted drug delivery to mesothelioma cells using functionally selected internalizing human single-chain antibodies. Mol Cancer Ther 2008;7:569–578. [PubMed: 18319332]
21. Bidlingmaier S, He J, Wang Y, An F, Feng J, Barbone D, et al. Identification of MCAM/CD146 as the Target Antigen of a Human Monoclonal Antibody that Recognizes Both Epithelioid and Sarcomatoid Types of Mesothelioma. Cancer Res 2009;69:1570–1577. [PubMed: 19221091]
22. Liu B, Conrad F, Cooperberg M, Kirpotin D, Marks J. Mapping tumor epitope space by direct selection of single-chain Fv antibody libraries on prostate cancer cells. Cancer Res 2004;64:704–710. [PubMed: 14744788]
23. MacDonald R, MacDonald R, Menco B, Takeshita K, Subbarao N, Hu L. Small-volume extrusion apparatus for preparation of large, unilamellar vesicles. Biochim Biophys Acta 1991;1061:297–303. [PubMed: 1998698]
24. Bartlett G. Phosphorus assay in column chromatography. J Biol Chem 1959;234:466–468. [PubMed: 13641241]
25. Kirpotin D, Park J, Hong K, Zalipsky S, Li W, Carter P, et al. Sterically stabilized anti-HER2 immunoliposomes: design and targeting to human breast cancer cells in vitro. Biochemistry 1997;36:66–75. [PubMed: 8993319]

26. Park J, Hong K, Kirpotin D, Colbern G, Shalaby R, Baselga J, et al. Anti-HER2 immunoliposomes: enhanced efficacy attributable to targeted delivery. Clin Cancer Res 2002;8:1172–1181. [PubMed: 11948130]
27. Iden D, Allen T. In vitro and in vivo comparison of immunoliposomes made by conventional coupling techniques with those made by a new post-insertion approach. Biochim Biophys Acta 2001;1513:207–216. [PubMed: 11470092]
28. Ellman G. Tissue sulfhydryl groups. Arch Biochem Biophys 1959;82:70–77. [PubMed: 13650640]
29. Mougin-Degraef M, Bourdeau C, Jestin E, Saï-Maurel C, Bourgeois M, Saëc PR, et al. Doubly radiolabeled liposomes for pretargeted radioimmunotherapy. Int J Pharm 2007;344:110–117. [PubMed: 17592745]
30. Dhalluin X, Scherpereel A. Treatment of malignant pleural mesothelioma: current status and future directions. Monaldi Arch Chest Dis 2010;73:79–85. [PubMed: 20949774]
31. Skubitz K. Phase II Trial of Pegylated-Liposomal Doxorubicin (Doxil) in Mesothelioma 1. Cancer Invest 2002;20:693–699. [PubMed: 12197225]
32. Steele J, O'Doherty C, Shamash J, Evans M, Gower N, Tischkowitz M, et al. Phase II trial of liposomal daunorubicin in malignant pleural mesothelioma. Ann Oncol 2001;12:497–499. [PubMed: 11398882]
33. Baas P, Van Meerbeeck J, Groen H, Schouwink H, Burgers S, Daamen S, et al. Caelyx™ in malignant mesothelioma: A phase II EORTC study. Ann Oncol 2000;11:697–700. [PubMed: 10942058]
34. Lu C, Perez-Soler R, Piperdi B, Walsh G, Swisher S, Smythe W, et al. Phase II study of a liposome-entrapped cisplatin analog (L-NDDP) administered intrapleurally and pathologic response rates in patients with malignant pleural mesothelioma. J Clin Oncol 2005;23:3495–501. [PubMed: 15908659]
35. Park J, Hong K, Kirpotin D, Papahadjopoulos D, Benz CC. Immunoliposomes for cancer treatment. Adv Pharmacol 1997;40:399–435. [PubMed: 9217932]
36. Kontermann R. Immunoliposomes for cancer therapy. Curr Opin Mol Ther 2006;8:39–45. [PubMed: 16506524]
37. Hertlein E, Triantafillou G, Sass EJ, Hessler JD, Zhang X, Jarjoura D, et al. Milatuzumab immunoliposomes induce cell death in CLL by promoting accumulation of CD74 on the surface of B cells. Blood 2010;116:2554–2558. [PubMed: 20574049]
38. Moase E, Qi W, Ishida T, Gabos Z, Longenecker B, Zimmermann G, et al. Anti-MUC-1 immunoliposomal doxorubicin in the treatment of murine models of metastatic breast cancer. Biochim Biophys Acta 2001;1510:43–55. [PubMed: 11342146]
39. Park J, Hong K, Carter P, Asgari H, Guo L, Keller G, et al. Development of anti-p185HER2 immunoliposomes for cancer therapy. Proc Natl Acad Sci U S A 1995;92:1327–1331. [PubMed: 7877976]
40. Bendas G. Immunoliposomes: a promising approach to targeting cancer therapy. BioDrugs 2001;15:215–224. [PubMed: 11437687]
41. Szoka F Jr, Papahadjopoulos D. Comparative properties and methods of preparation of lipid vesicles (liposomes). Annu Rev Biophys Bioeng 1980;9:467–508. [PubMed: 6994593]
42. Templeton N, Lasic D. New directions in liposome gene delivery. Mol Biotechnol 1999;11:175–180. [PubMed: 10464771]
43. Barenholz Y. Liposome application: problems and prospects. Curr Opin Colloid Interface Sci 2001;6:66–77.
44. Hansen C, Kao G, Moase E, Zalipsky S, Allen T. Attachment of antibodies to sterically stabilized liposomes: evaluation, comparison and optimization of coupling procedures. Biochim Biophys Acta 1995;1239:133–144. [PubMed: 7488618]
45. Allen T, Agrawal A, Ahmad I, Hansen C, Zalipsky S. Antibody-mediated targeting of long-circulating (stealth) liposomes. J Liposome Res 1994;4:1–25.
46. Maruyama K, Takizawa T, Yuda T, Kennel S, Huang L, Iwatsuru M. Targetability of novel immunoliposomes modified with amphipathic poly (ethylene glycol) s conjugated at their distal terminals to monoclonal antibodies. Biochim Biophys Acta 1995;1234:74–80. [PubMed: 7880861]

47. Martin F, Hubbell W, Papahadjopoulos D. Immunospecific targeting of liposomes to cells: a novel and efficient method for covalent attachment of Fab' fragments via disulfide bonds. Biochemistry 1981;20:4229–4238. [PubMed: 7284322]

48. Moreira J, Ishida T, Gaspar R, Allen T. Use of the post-insertion technique to insert peptide ligands into pre-formed stealth liposomes with retention of binding activity and cytotoxicity. Pharm Res 2002;19:265–269. [PubMed: 11934232]

49. Scatchard G. The attraction of proteins for small molecules. Ann NY Acad Sci 1949;51:660–672.

50. Sullivan S, Huang L. Preparation and characterization of heat-sensitive immunoliposomes. Biochim Biophys Acta 1985;812:116–126. [PubMed: 3967009]

51. Babbitt B, Huang L. Effects of valency on thermodynamic parameters of specific membrane interaction. Biochemistry 1985;24:2186–2194. [PubMed: 3995009]

52. Heath T, Fraley R, Bentz J, EW V Jr, Herron J, Papahadjopoulos D. Antibody-directed liposomes Determination of affinity constants for soluble and liposome-bound antifluorescein. Biochim Biophys Acta 1984;770:148–158. [PubMed: 6421325]

53. Maruyama K, Kennel S, Huang L. Lipid composition is important for highly efficient target binding and retention of immunoliposomes. Proc Natl Acad Sci U S A 1990;87:5744–5748. [PubMed: 2377612]

54. Ahmad I, Allen T. Antibody-mediated specific binding and cytotoxicity of liposome-entrapped doxorubicin to lung cancer cells in vitro. Cancer Res 1992;52:4817–4820. [PubMed: 1511445]

55. Mishra S, Webster P, Davis M. PEGylation significantly affects cellular uptake and intracellular trafficking of non-viral gene delivery particles. Eur J Cell Biol 2004;83:97–111. [PubMed: 15202568]

56. Hong R, Huang C, Tseng Y, Pang V, Chen S, Liu J, et al. Direct Comparison of Liposomal Doxorubicin with or without Polyethylene Glycol Coating in C-26 Tumor-bearing Mice. Clin Cancer Res 1999;5:3645–3652. [PubMed: 10589782]

57. Torchilin V, Klibanov A, Huang L, O'Donnell S, Nossiff N, Khaw B. Targeted accumulation of polyethylene glycol-coated immunoliposomes in infarcted rabbit myocardium. FASEB J 1992;6:2716–2719. [PubMed: 1612296]

58. De Menezes L, Daniel E, Pilarski L, Allen T. In vitro and in vivo targeting of immunoliposomal doxorubicin to human B-cell lymphoma. Cancer Res 1998;58:3320–3330. [PubMed: 9699662]

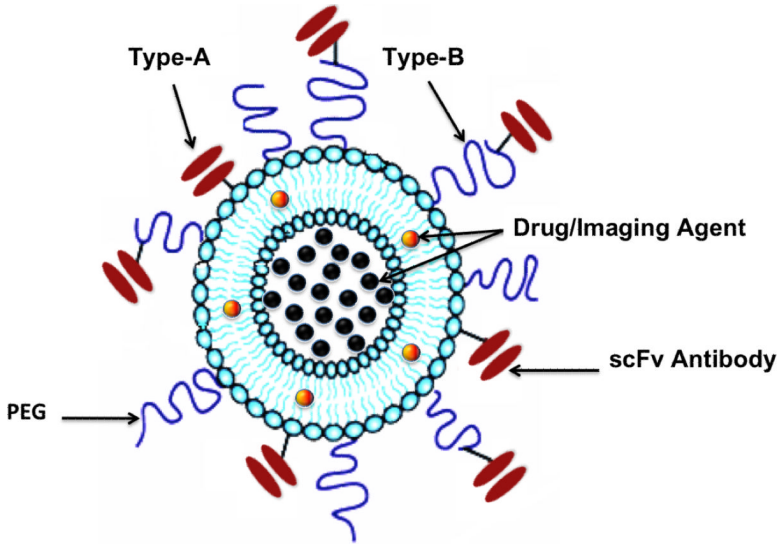

Figure 1. A schematic of multifunctional sterically stabilized long circulating immunoliposome
The figure shows two modes of conjugating the scFv antibody to the liposome; in Type A immunolipsome the scFv antibody is directly conjugated onto the liposome whereas in Type B immunoliposome, the scFv antibody is conjugated onto the liposome *via* a flexible spacer (such as DSPE-PEG).

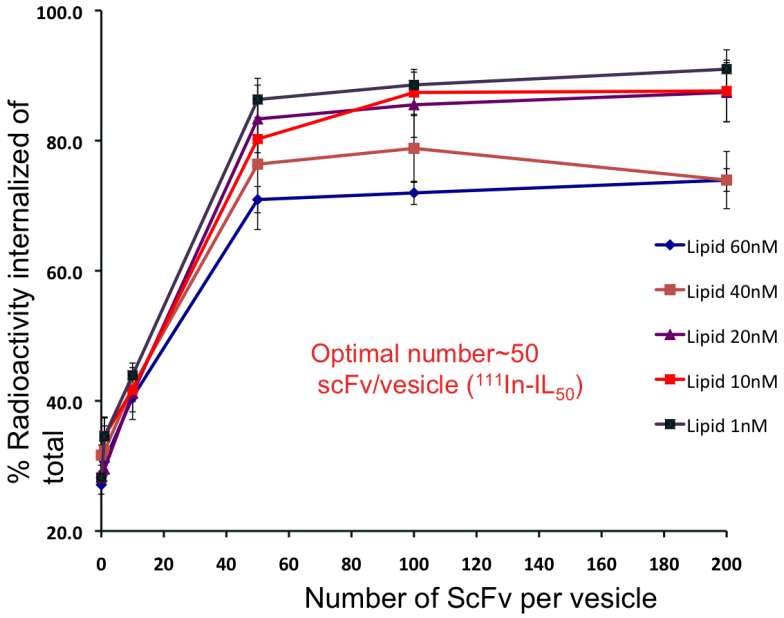

Figure 2. ***In vitro*** **internalization of ^{111}In-IL-M1 in VAMT-1 cells**

The internalization of ^{111}In-IL-M1 was tested with varied number of M1 scFv *per* liposome ranging from 1 to 200 scFv *per* vesicle and at varied lipid concentrations from 1 nM to 60 nM as shown, on VAMT-1 cells incubated at 37°C for 24 h (n=4).

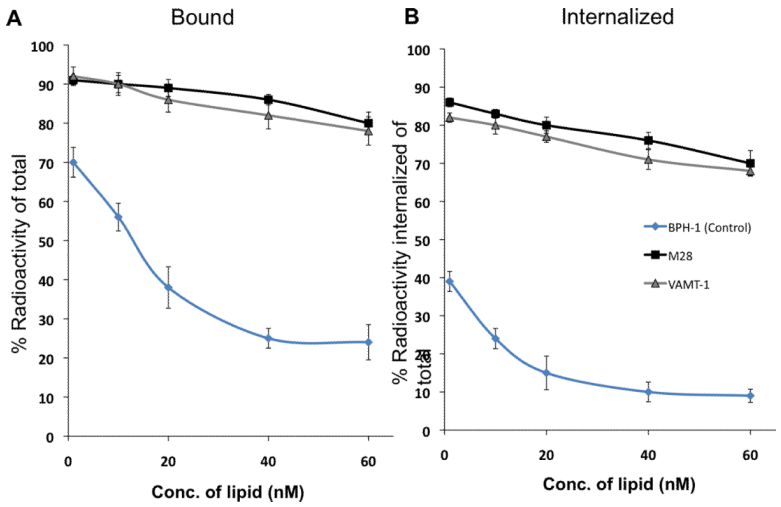

Figure 3. ***In vitro*** **cell binding (A) and internalization (B) curves**

Binding and internalization of ^{111}In-IL-M1$_{50}$ on M28 (black), VAMT-1 (grey) and control BPH-1 cells (blue) at 37°C after 24 h incubation period are shown (n=3).

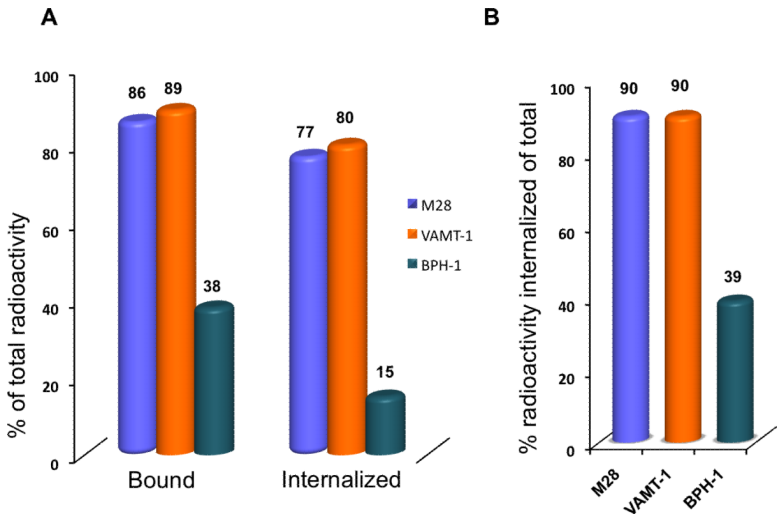

Figure 4. Comparative IL uptake in tumor and normal cells

A. Comparison of *in vitro* binding and internalization of ^{111}In-IL-M1$_{(50)}$ in mesothelioma tumor cells (M28, VAMT-1) and normal (BPH-1) cells; **B.** The percentage radioactivity internalized (of the total) into tumor cells and normal cells are shown. The cells were incubated with ^{111}In-IL-M1$_{(50)}$ with a lipid concentration of 20 nM at 37°C for 24 h.

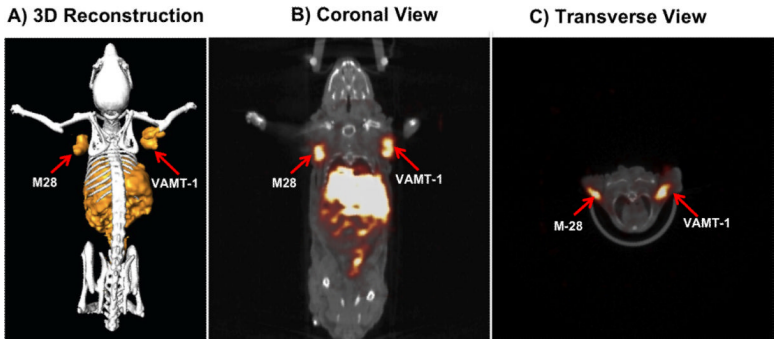

Figure 5. SPECT/CT Imaging

SPECT/CT fused image of ^{111}In-IL-M1$_{(50)}$ taken 24 h after injection; **A)** 3-Dimensional Reconstruction; **B)** Coronal view; **C)** Transverse view. The uptake of ^{111}In-IL-M1$_{(50)}$ in both epithelioid (M28) and sarcomatoid (VAMT-1) mesothelioma tumors at 24 h is clearly seen.

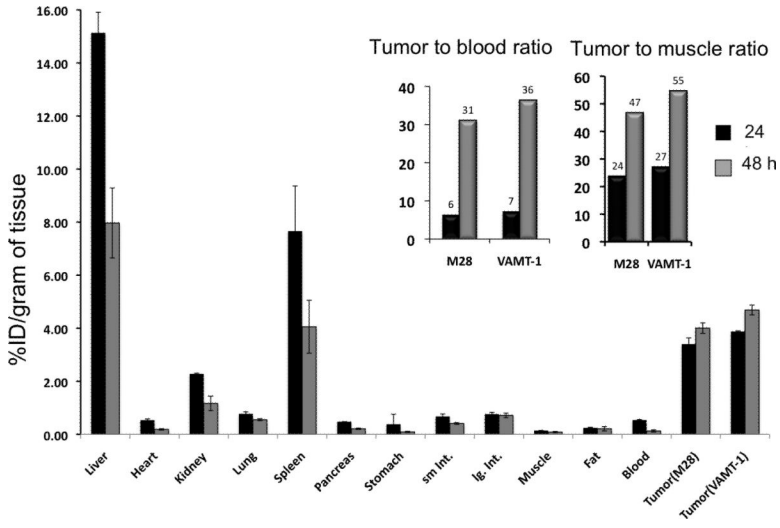

Figure 6. Biodistribution of ILs

Biodistribution of ^{111}In-IL-M1$_{(50)}$ at 24 h and 48 h in mice bearing both epithelioid (M28) and sarcomatoid (VAMT-1) tumors are shown (n=4). **Inset:** The tumor to blood and tumor to muscle ratios of ^{111}In-IL-M1$_{(50)}$ at 24 h and 48 h in M28 and VAMT-1 tumors are shown.

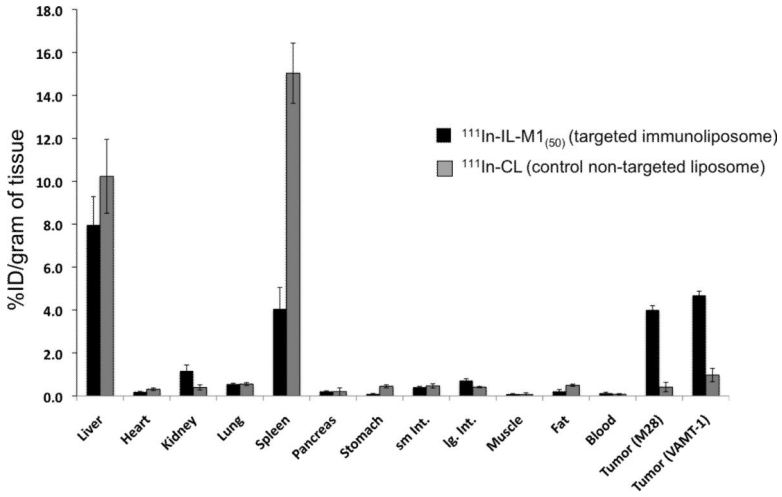

Figure 7. Comparison of targeted and non-targeted liposome uptake *in vivo*

48 h biodistribution of targeted ILs (^{111}In-IL-M1$_{(50)}$) versus control non-targeted immunoliposome (^{111}In-CL) in mice bearing both epithelioid (M28) and sarcomatoid (VAMT-1) tumors are shown (n=3).

Table 1

Concentration of liposome (lipid) to scFvs ratios to obtain varied number of scFv *per* vesicle is shown.

Lipid conc.	No. of vesicles*	ScFv conc.	No. of ScFv	No of scFv / vesicle
150 mM (100 μl)	10^{14}	5 μg	10^{14}	1
15 mM (100 μl)	10^{13}	5 μg	10^{14}	10
3 mM (100 μl)	2×10^{12}	5 μg	10^{14}	50
1.5 mM (100 μl)	10^{12}	5 μg	10^{14}	100
0.75 mM (100 μl)	5×10^{11}	5 μg	10^{14}	200

* Based on an assumption that 100 nm size liposomes form unilamellar vesicles.

Table 2

Hydrodynamic size and zeta potentials of non-targeted and M1 scFv targeted immunoliposome are shown. IL-$M1_{(50)}$ and IL-$M1_{(100)}$ are the M1-scFv targeted immunoliposome inserted with 50 and 100 scFv *per* vesicle respectively.

Liposome formulation	Hydrodynamic diameter (nm)	Zeta potentials (mV)
Non-targeted control liposome	97.3 ± 4.60	-18 ± 2.23
IL- $M1_{(50)}$	109.7± 3.86	-20 ± 4.32
IL- $M1_{(100)}$	117.3± 3.35	-23 ± 3.86

TABLE 3

Biodistribution of ^{111}In-IL-M1$_{(50)}$ (at 24 and 48 h after injection) in nude mice bearing both epithelioid (M28) and sarcomatoid (VAMT-1) subtypes of mesothelioma tumors (n=4). A control study performed using non-targeted ^{111}In-CL is also shown (n=3). Data are %ID/g ± SD.

Organ	^{111}In-IL-M1$_{(50)}$		Control ^{111}In-CL
	24 h	48 h	48 h
Liver	15.69±2.28	7.97±0.34	10.23±0.11
Heart	0.57±0.13	0.19±0.13	0.31±0.11
Kidney	2.26±1.24	1.17±2.75	1.40±0.51
Lung	0.72±0.33	0.55±0.24	0.55±0.29
Spleen	8.87±0.91	4.06.±086	5.04±0.89
Pancreas	0.48±0.18	0.21±0.23	0.20±0.56
Stomach	0.12±0.78	0.69±0.68	0.45±0.66
Sm. Int.	0.74±0.89	0.41±0.98	0.47±0.91
Ig. Int.	0.71±0.92	0.72±0.91	0.41±0.93
Muscle	0.14±0.02	0.09±0.05	0.07±0.01
Fat	0.23±0.01	0.21±0.03	0.10±0.02
Blood	0.53±0.21	0.13±0.63	0.50±0.58
Tumor (M28)	3.24±0.24	4.01±0.39	0.97±0.48
Tumor (VAMT-1)	3.86±0.23	4.69±0.72	0.40±0.42